Studies of Mg^{25}, Mg^{26}, and Mg^{27} Nuclei With (d,p) Reactions*

Bibijana Ćujec†

University of Pittsburgh, Pittsburgh, Pennsylvania

(Received 1 June 1964)

By irradiating Mg^{24}, Mg^{25}, and Mg^{26} targets with 15-MeV deuterons, the proton spectra have been measured at four angles up to high excitation energies of the residual nuclei, and as a result many new levels of Mg^{25}, Mg^{26}, and Mg^{27} have been identified in the region above the neutron separation energy. The 3.969-MeV level of Mg^{25} and the two unresolved levels of Mg^{27} at 3.76 MeV and 3.78 MeV have angular distributions characteristic of $l=3$ angular-momentum transfer rather than of $l=2$. Detailed consideration has been given to the low-lying levels and to the applicability of the distorted-wave Born-approximation (DWBA) method in calculating the single-particle cross sections. From stripping cross sections and related spectroscopic factors, evidence has been obtained that the low-lying levels of Mg^{26} and Mg^{27} may be considered as members of rotational bands, analogous to those of Mg^{24} and Mg^{25}, respectively.

INTRODUCTION

AN appreciable amount of information has already been gathered about magnesium nuclei. Thus the energy levels have been located by Hinds, Marchant, and Middleton[1] in Mg^{25} up to 7.64 MeV, in Mg^{26} up to 10.515 MeV, and in Mg^{27} up to 7.031 MeV, using various reactions. These and previous data are summarized by Endt and Van der Leun.[2] Sheline and Harlan[3] located levels in Mg^{25} up to 8.7 MeV, using the reaction $Al^{27}(d,\alpha)Mg^{25}$. Recently, Middleton and Hinds[4] measured the angular distribution (from 0° to 180°) of protons from the $Mg^{24}(d,p)Mg^{25}$ reaction, initiated with 10-MeV deuterons, for all levels of Mg^{25} up to 7.40 MeV. They found that some of the levels do not show a characteristic stripping pattern, but have rather isotropic angular distributions. The other angular distributions have been successfully fitted with Butler curves (all with the same radius); the l values assigned agree with previous[2] determinations (Table I). Less information[2] about the l values of the transferred neutron exists for the $Mg^{26}(d,p)Mg^{27}$ reaction; it is based on the work of Hinds, Middleton, and Parry[5] and on unpublished work of Parkinson.[6] The assignment of l values for the $Mg^{25}(d,p)Mg^{26}$ reaction is more difficult because in general more than one l value occurs in transitions to individual levels. The assigned[2] l values are doubtful. Weinberg et al.,[7] for example, found that both $l=0$ and $l=2$ contribute to the transitions to the 1.81-, 2.94-, 3.94-, and 4.33-MeV excited states of Mg^{26}.

The aim of the present investigation was to get more information about the levels of Mg^{26} and Mg^{27} and to establish, if possible, the rotational bands, which have been already identified[2,8-11] in the neighboring nuclei Mg^{24}, Mg^{25}, Al^{25}, and Al^{27}. The stripping reactions provide very direct information about the wave function of the final state, especially when the spectroscopic factor can be extracted from the measured cross section. For rotational states, Satchler[12] has derived explicit relations between the spectroscopic factors and the coefficients c_{Nlj}^2, in terms of which the wave function of the captured neutron is given. On the other hand, coefficients c_{Nlj}^2 are uniquely predicted by Nilsson model[13] provided that the deformation is given. Thus one can easily check the applicability of the model to individual levels.

Accordingly, the present work puts emphasis on the measurement of cross sections and on calculation of the single-particle cross sections, which are needed to extract spectroscopic factors. The single-particle cross sections were calculated by the DWBA method. The applicability of this method to light nuclei and its limitations are discussed.

MEASUREMENTS AND RESULTS

The isotopes Mg^{24}, Mg^{25}, and Mg^{26} were bombarded with 15-MeV deuterons from the University of Pittsburgh cyclotron. The respective targets were 0.78 mg/cm², 0.75 mg/cm², and 0.50 mg/cm² thick. The outgoing protons were analyzed by the magnetic spectrometer and detected with photographic plates. The resolution was about 20 keV. The spectra show well-resolved peaks even in the region where the excitation energy of the residual nucleus becomes larger than the

* Supported by the U. S. Office of Naval Research and National Science Foundation.

† Present address: Department of Physics, Laval University, Quebec, Canada.

[1] S. Hinds, H. Marchant, and R. Middleton, Proc. Phys. Soc. (London) 78, 473 (1961).

[2] P. M. Endt and C. Van der Leun, Nucl. Phys. 34, 1 (1962).

[3] R. K. Sheline and R. A. Harlan, Nucl. Phys. 29, 177 (1962).

[4] R. Middleton and S. Hinds, Nucl. Phys. 34, 404 (1962).

[5] S. Hinds, R. Middleton, and G. Parry, Proc. Phys. Soc. (London) 71, 49 (1958).

[6] W. C. Parkinson, Bull. Am. Phys. Soc. 6, 259 (1961), and private communication.

[7] R. B. Weinberg, G. E. Mitchell, and L. J. Lidofsky, Phys. Rev. 133, B884 (1964).

[8] A. V. Cohen and J. A. Cookson, Nucl. Phys. 29, 604 (1962).

[9] A. E. Litherland, H. McManus, E. B. Paul, D. A. Bromley, and H. E. Gove, Can. J. Phys. 36, 378 (1958).

[10] A. E. Litherland, H. E. Gove, and A. J. Ferguson, Phys. Rev. 114, 1312 (1959); A. E. Litherland, E. B. Paul, G. A. Bartolomew, and H. E. Gove, ibid. 102, 208 (1956); H. E. Gove, A. E. Litherland, E. Almquist, and D. A. Bromley, ibid. 111, 608 (1958).

[11] E. Almquist, D. A. Bromley, H. E. Gove, and A. E. Litherland, Nucl. Phys. 19, 1 (1960).

[12] G. R. Satchler, Ann. Phys. (N. Y.) 3, 277 (1957).

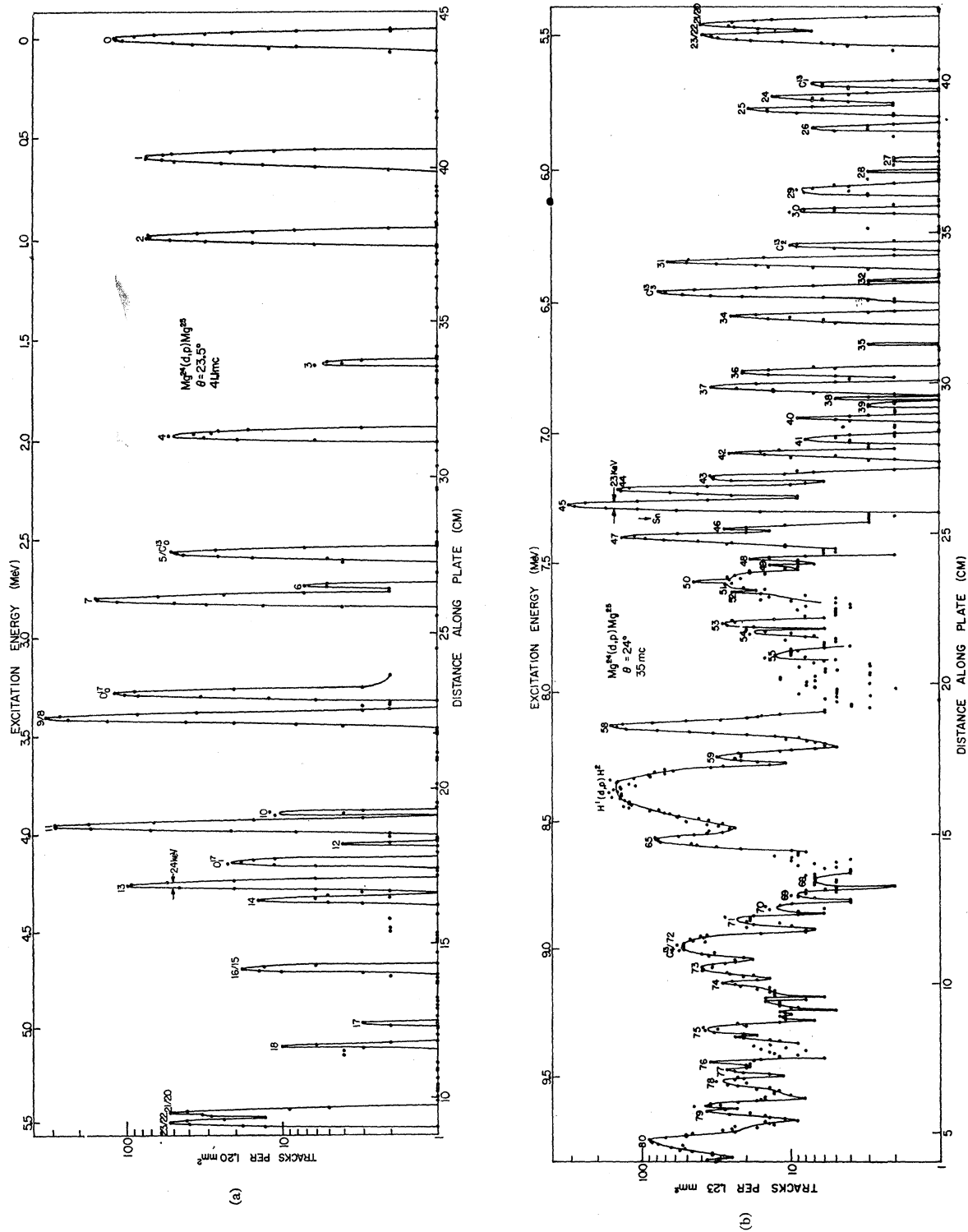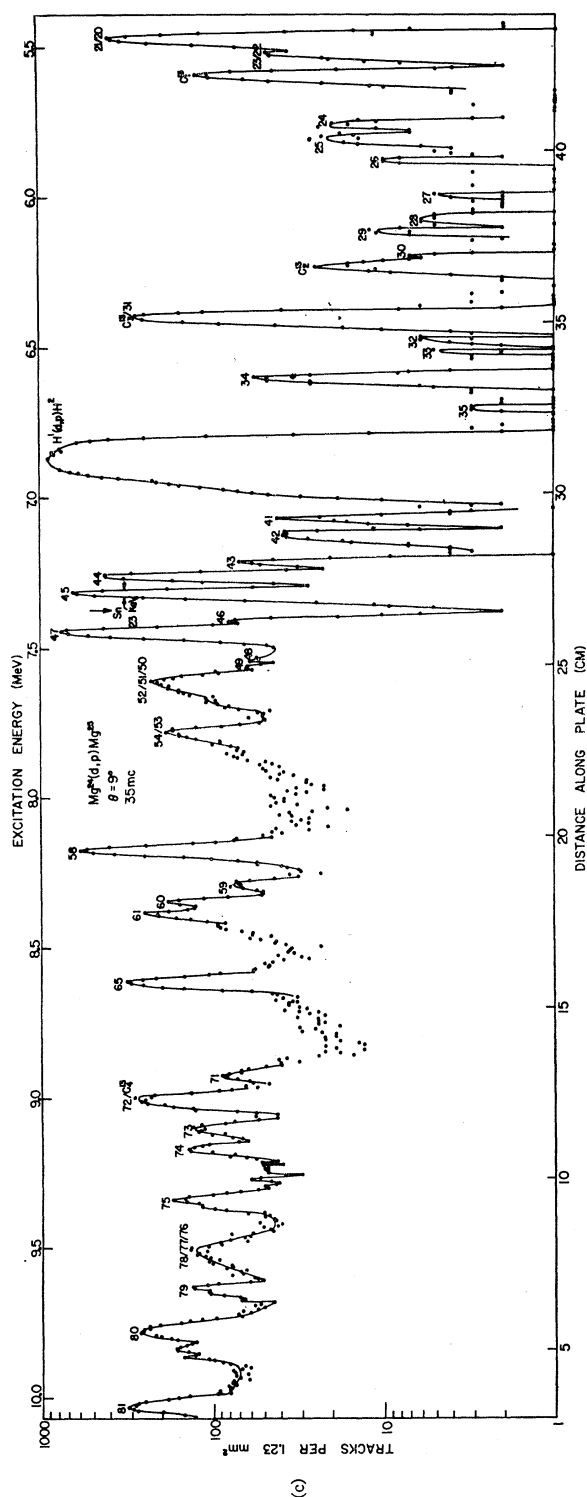[13] S. G. Nilsson, Kgl. Danske Videnskab. Selskab, Mat. Fys. Medd. 29, No. 16 (1955).

FIG. 1. Energy spectra of protons from reaction $Mg^{24}(d,p)Mg^{25}$. The upper abscissa shows the excitation energy of Mg^{25}. The separation energy of Mg^{25} ($S_n = 7.33$ MeV) is also marked.

neutron separation energy ($S_n = 7.331$ MeV for Mg^{25}, 11.111 MeV for Mg^{26}, and 6.437 MeV for Mg^{27}), i.e., in the beginning of the continuum region. To obtain the whole spectrum, showing well-resolved peaks, two different settings of the magnetic field (measured by the proton magnetic resonance frequency) had to be used with each of the reactions Mg$^{24}(d,p)$Mg^{25} and Mg$^{26}(d,p)$-Mg^{27}, and three with the reaction Mg$^{25}(d,p)$Mg^{26}.

The proton spectra were recorded at laboratory angles of 9°, 16°, 24°, and 38°. Some of the proton spectra obtained are shown on Figs. 1 to 3. For the continuum region, where many new levels have been located, the spectra are shown both at 9° and 24°; for the lower excitation energies, however, they are shown only at 24°.

The numerical results are presented in Table I, which includes also all previous data about energy levels, their spin values, and the l values of the stripped neutron. No attempt has been made to redetermine the position of energy levels in the region where these are already known. The absolute values of (d,p) cross sections, leading to the respective energy levels of the residual nucleus, are quoted at $\theta = 25°$ (c.m. system). The information about the angular distribution is presented in the last three columns, where the cross sections at 10°, 15°, and 40° (c.m. system) are given relative to the cross section at 25° (cross section at 25° equals unity). On the basis of this information some new assignments of the l values were possible (see next section).

In the continuum region, where some new levels have been located, there exists also a continuous spectrum of protons arising from the breakup of a deuteron into a neutron and a proton. The intensity of this background is increasing with decreasing proton energy and with decreasing angle of observation. Because of this background only the levels with large (d,p) cross section could be located. Some of the peaks very probably represent groups of two or more unresolved levels.

DISTORTED-WAVE BORN APPROXIMATION

The distorted-wave Born-approximation (DWBA) method or so-called optical model analysis has been very successfully applied in this laboratory to stripping reactions on a variety of heavy and medium weight nuclei. With optical model parameters obtained from elastic scattering data, good fits were obtained[14] to angular distributions up to about 90°. Also, in this region the single-particle cross sections are predicted correctly, which is proved by the fact that the sum rules for spectroscopic factors are fulfilled.

With light nuclei, experimental physicists still prefer[15] to apply—apparently for reasons of simplicity—the plane-wave Butler theory, which fits the angular distributions quite well but gives—as is well known—too

[14] B. L. Cohen and O. V. Chubinsky, Phys. Rev. **131**, 2184 (1963).
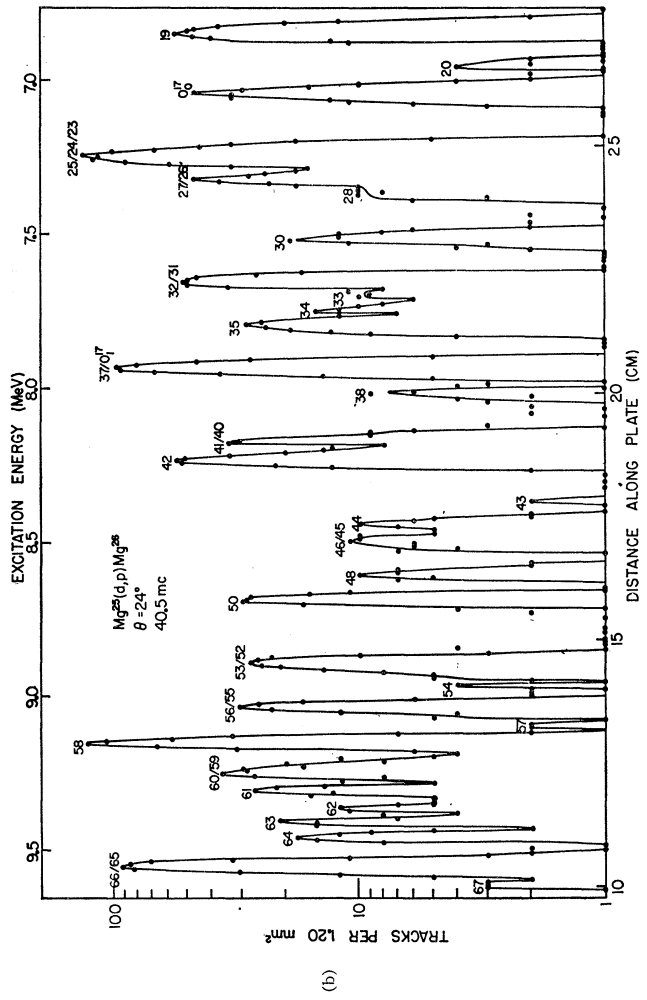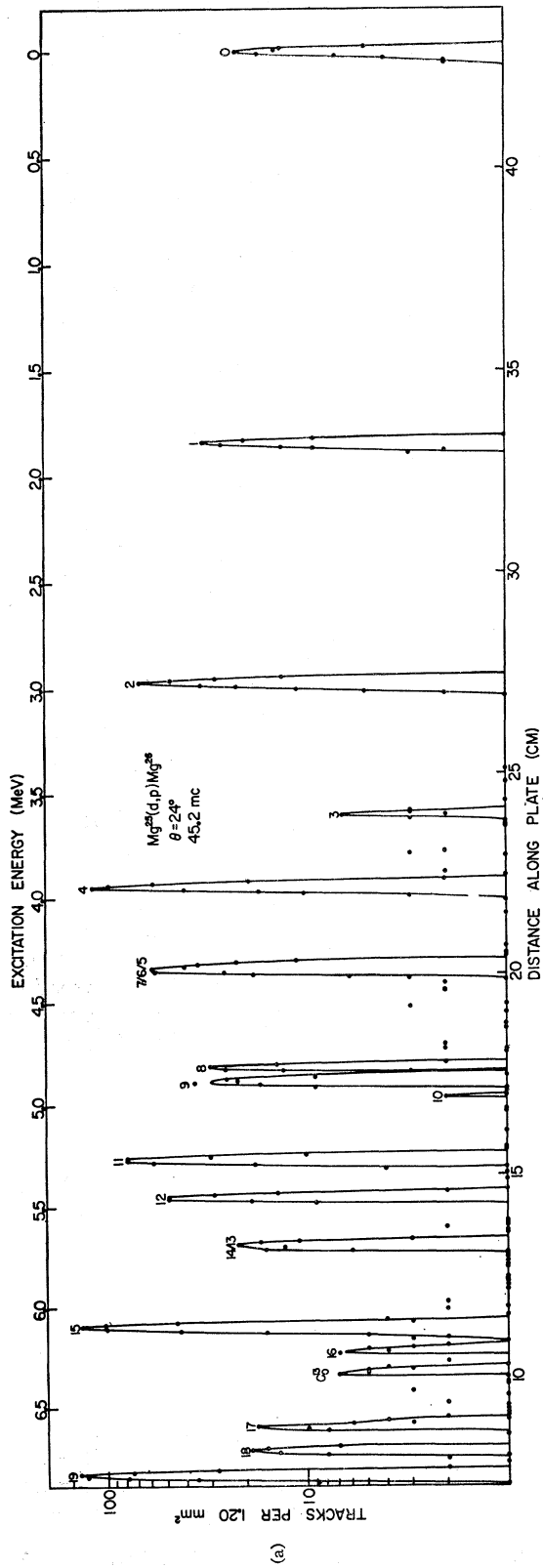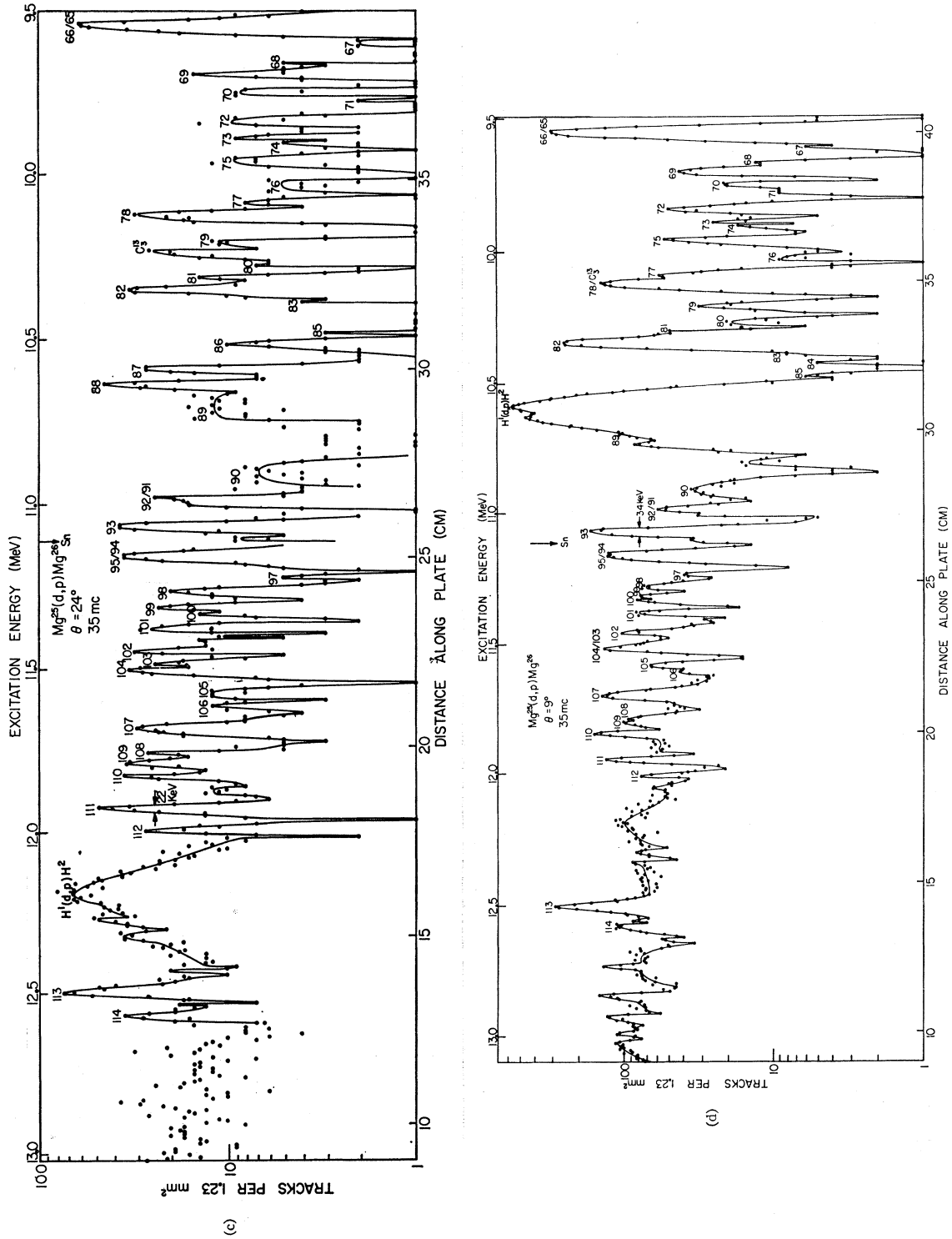[15] See, e.g., Ref. 4.

FIG. 2.

FIG. 2. Energy spectra of protons from reaction Mg²⁵(d,p)Mg²⁶. The upper abscissa shows the excitation energy of Mg²⁶. The separation energy of Mg²⁶ (Sₙ = 11.11 MeV) is also marked.
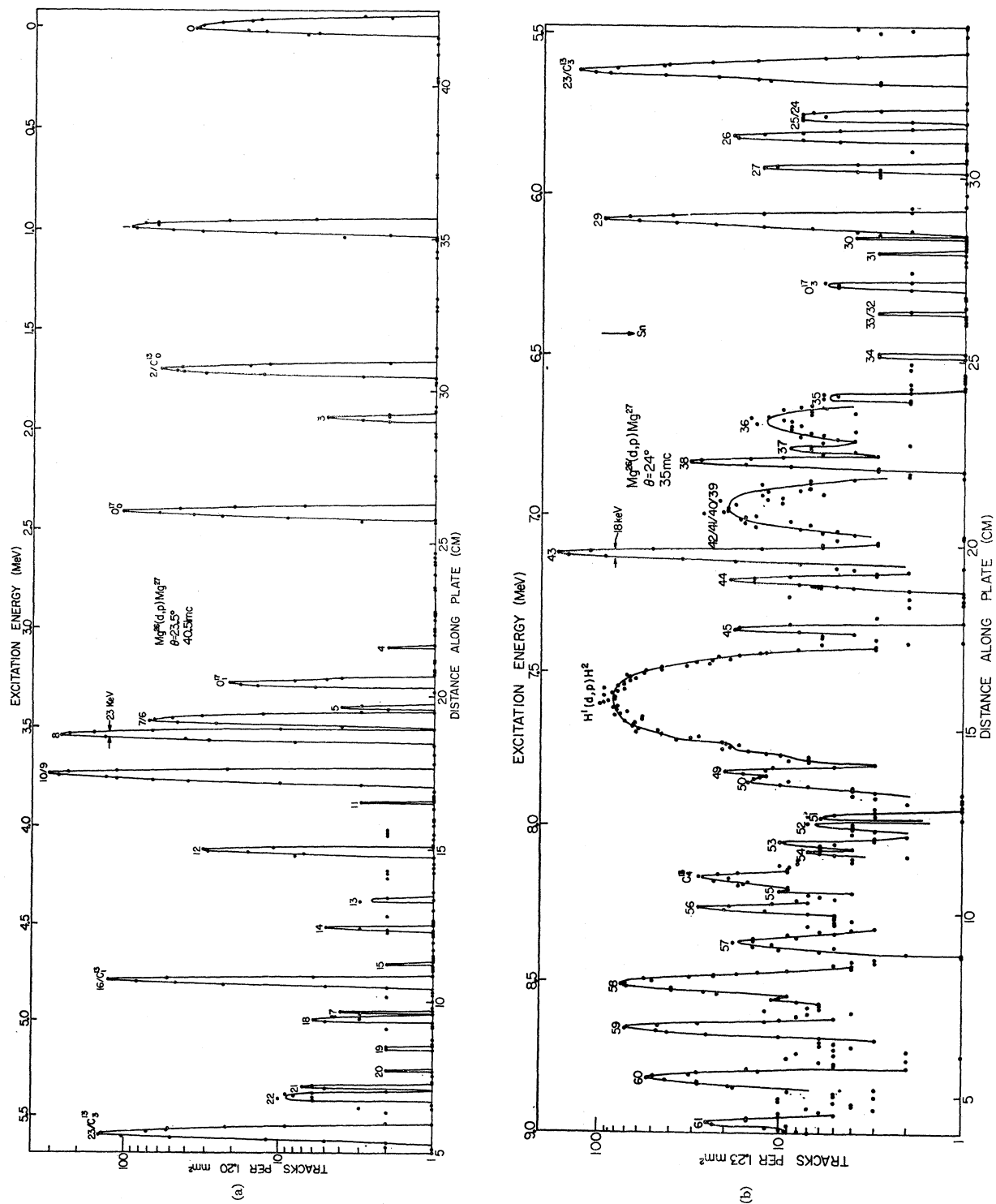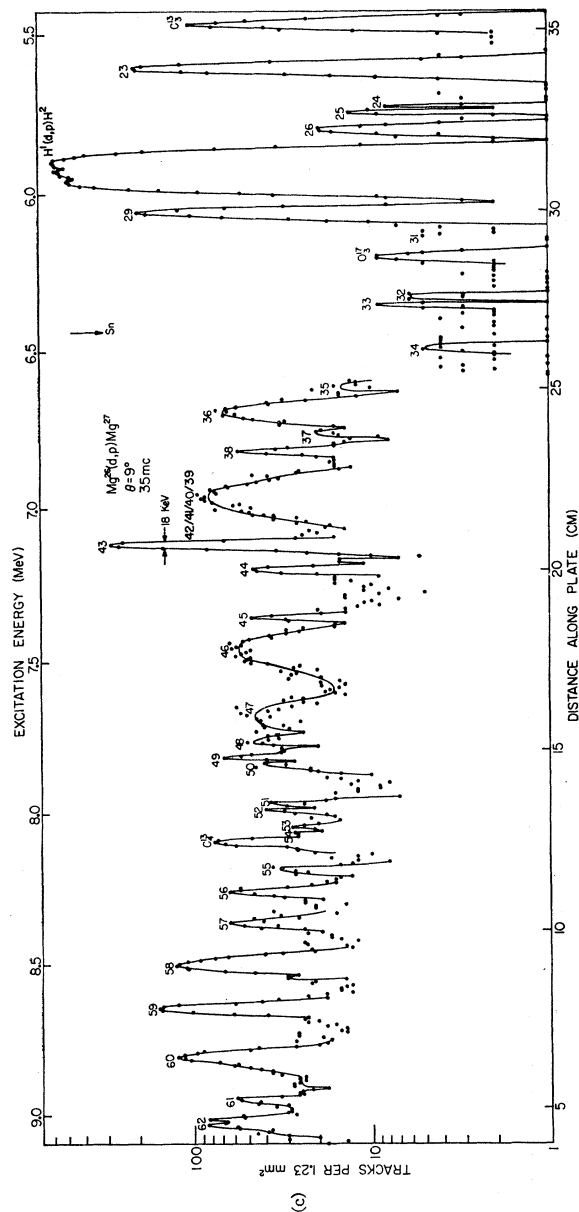
FIG. 3.

FIG. 3. Energy spectra of protons from reaction $Mg^{26}(d,p)Mg^{27}$. The upper abscissa shows the excitation energy of Mg^{27}. The separation energy of Mg^{27} ($S_n = 6.44$ MeV) is also marked.

large single-particle cross sections. The difficulty can be overcome if one factor, the so-called single-particle reduced width θ_0^2, is obtained from some other experiment, for which the spectroscopic factor is known. In most cases, however, the results are given as products of spectroscopic factor and single-particle reduced width $(S\theta_0^2)$ expressed relatively to the ground state transition $(S\theta_0^2 = 1$ for ground state). As the reduced widths θ_0^2 depend on many variables, especially on the l value and on the neutron binding energy, little information is obtained in that way about the spectroscopic factors themselves. Although the estimates of reduced widths θ_0^2 by Macfarland and French[16] are of some help, a more accurate approach is highly desirable.

The most natural approach is the application of DWBA. Very encouraging here is the fact that the theory has predicted correctly the cross sections for (d,He^3) reactions in d-s shell nuclei.[17] As with the previous DWBA calculations used in this laboratory, the optical model parameters were adopted from the elastic scattering data. The code JULIE, written by Bassel, Drisko, and Satchler[18] was used, and the integration performed over the whole region (without lower cut-off). The optical potentials adopted have the same form as in the analysis of elastic scattering; numerical values of parameters are given in Table II.

Recently two other DWBA calculations were applied to the $Mg^{24}(d,p)Mg^{25}$ ground state $(l=2)$ and first excited state $(l=0)$. Buck and Hodgson[19] applied it to angular distributions measured by Middleton and Hinds[4] at $E_d = 10$ MeV. Smith and Ivash,[20] trying a systematic approach to light nuclei in general, applied it to the same two experimental angular distributions of Middleton and Hinds[4] and to the $Mg^{24}(d,p)Mg^{25}$ ground-state angular distribution measured by Hamburger and Blair[21] at $E_d = 15$ MeV. Both these approaches differ from the present one in the way that the depths of the optical potentials (V and W) were adjusted to the stripping data. Smith and Ivash adjust them to each angular distribution separately, while Buck and Hodgson adjust them only to one angular distribution (leading to the first excited state of Mg^{25}) and keep them constant in calculating the other (leading to the ground state of Mg^{25}). Smith and Ivash pointed out that the imaginary potentials W obtained from elastic-scattering data are generally appreciably larger than these derived from stripping measurements. Smaller W give larger stripping cross sections with backward angles in better agreement with experiment. High values of W in the analysis of elastic scattering data become unnecessary if the spin-orbit interaction is included.

[16] M. H. Macfarlane and J. B. French, Rev. Mod. Phys. 32, 567 (1960).
[17] B. Čujec, Phys. Rev. 128, 2303 (1962).
[18] R. H. Bassel, R. M. Drisko, and G. R. Satchler, Oak Ridge National Lab. Report ORNL-3240 (unpublished).
[19] B. Buck and P. E. Hodgson, Nucl. Phys. 29, 496 (1962).
[20] W. R. Smith and E. V. Ivash, Phys. Rev. 131, 304 (1963).
[21] E. W. Hamburger and A. G. Blair, Phys. Rev. 119, 777 (1960).

TABLE I. Energy levels of Mg isotopes and cross sections for (d,p) reactions initiated with 15-MeV deuterons.

(1)	(2)	(3)	(4)	(5)	(6)	(7)
					$\dfrac{d\sigma}{d\Omega}$ relative[i] to $\dfrac{d\sigma}{d\Omega}$ (25°)	
Group number[a]	Energy level[b] (MeV)	l[b]	$d\sigma/d\Omega(25°)$[e] (mb/sr)	10°	15°	40°
	Mg²⁵			Mg²⁴(d,p)Mg²⁵		
0	0 5/2⁺	2, 2[d]	3.98	1.32	1.12	0.30
1	0.584 1/2⁺	0, 0[d]	2.58	>3.42	2.43	0.76
2	0.976 3/2⁺	2, 2[d]	2.15	1.10	0.94	0.16
3	1.611 (7/2)⁺	(2), ...[d]	0.10	0.8	1.0	0.6
4	1.962 5/2⁺	2, 2[d]	1.15	1.01	0.96	0.46
5	2.565 1/2⁺	0, 0[d]	0.85[e]	>7.5	3.98	0.53
6	2.737 (7/2⁺)[f]	...[d]	0.11	0.2	0.4	0.3
7	2.803 (3/2,5/2)⁺	2, 2[d]	3.05	1.18	1.24	0.21
8	3.399 (9/2⁺)	}1, 1[d]	small			
9	3.408 3/2⁻		5.66	>1.46	>1.22	0.41
10	3.903 (3/2,5/2)⁺	...[d]	0.13	1.4	1.1	0.2
11	3.969 (7/2⁻)[f]	(2,3),[d] 3[i]	5.19	~0.65	0.79	0.38
12	4.055 (9/2⁺)[f]	...[d]	0.04	~1.0	~1.0	~1.0
13	4.270 (1/2)⁻	1, 1[d]	1.59	3.46	3.10	0.72
14	4.351	...[d]	0.16	1.7	1.5	0.3
15	4.70	}(2),...[d]	0.30	1.7	1.5	0.2
16	4.72					
17	5.01	...[d]	0.04			
18	5.11	...[d]	0.07	2.1	1.9	
19	5.24	...[d]	0.02			
20	5.45	small[g]	}0.70	7.81	3.82	
21	5.47	0, 0[d] ~0.70[g]				
22	5.51	1 ~0.50[g]	}0.75	0.91	1.14	
23	5.52	(2) ~0.25[g]				
24	5.74	...[d]	0.18	1.6	0.9	
25	5.79	...[d]	0.27	1.3	1.4	
26	5.85	...[d]	0.08	1.4	0.9	
27	5.97	...[d]	0.02			
28	6.03	...[d]	0.02			
29	6.07	...[d]	0.17	0.7	1.0	
30	6.16	...[d]	0.10	C	1.2	
31	6.35	(2)[d]	0.95	C	1.75	
32	6.42	...[d]	0.02			
33	6.46	...[d]	~0.05			
34	6.56	(2), ...[d]	0.32	2.0	1.6	
35	6.67	...[d]	0.01			
36	6.77	1, 1[d]	0.34	H	2.4	
37	6.82	...[d]	0.53	H	1.4	
38	6.87	...[d]	0.03	H		
39	6.90	...[d]	0.04	H		
40	6.94	...[d]	0.09	H	1.8	
41	7.02	...[d]	0.10	3.3	2.0	
42	7.08	2, 2[d]	0.31	2.0	H	
43	7.17	...[d]	0.57	1.2	H	
44	7.21	2, 2[d]	2.06	2.23	H	
45	7.27	3, 3[d]	4.61	1.51	1.05	
46	7.37	2, 2[d]	0.25	2.7	1.5	
47	7.411 3/2⁻	1, 1[d]	2.13	4.69	2.58	
48	7.49		0.21			
49	7.51, 7.53[f]					
50	7.56, 7.57[f]					
51[h]	7.59 1/2⁻, Γ=80 keV	1	}1.61	4.46	3.07	
52	7.62, 7.63[f]					
53	7.744 7.74[i]		0.42	}4.50	3.00	
54	7.79,[f] 7.76[i]		0.34			
55	7.85, 7.85,[f] 7.85[i]		0.25			
56	8.01[f]					
57	8.05, 8.08[f]					
58	8.11,[f] 8.13[i]		3.09	2.44	1.95	
59	8.27,[f] 8.25[i]		0.50	1.66	1.05	
60	8.31,[f] 8.31[i]		1.10[j]			
61	8.36,[f] 8.35[i]		2.66[j]			
62	8.40[f]					
63	8.45[f]					
64	8.53[f]					
65	8.58,[f] 8.57[i]		1.81	2.25	1.84	
66	8.65[f]					
67	8.71[f]					

TABLE I (continued)

(1) Group number[a]	(2) Energy level[b] (MeV)	(3) l[b]	(4) $d\sigma/d\Omega(25°)$[c] (mb/sr)	(5) $\frac{d\sigma}{d\Omega}$ relative[i] to $\frac{d\sigma}{d\Omega}(25°)$ 10°	(6) 15°	(7) 40°
	Mg²⁵			**Mg²⁴(d,p)Mg²⁵**		
68	8.74[i]		0.12			
69	8.79[i]		0.12			
70	8.84[i]		0.13			
71	8.89[i]		0.38	2.86	2.40	
72	8.97[i]		<1.93	~2.27	~1.92	
73	9.07[i]		0.92	1.95	1.69	
74	9.13[i]		0.32	5.43	3.61	
75	9.32[i]		0.70	3.31	2.19	
76	9.45[i]		0.23			
77	9.48[i]		0.23	}3.02	2.03	
78	9.52[i]		0.45			
79	9.62[i]		0.64	2.37	1.64	
80	9.76[i]		2.14	2.08	1.68	
81	10.02[i]		3.26[j]			
	Mg²⁶			**Mg²⁵(d,p)Mg²⁶**		
0	0	0⁺	2	0.44	1.05		0.60
1	1.81	2⁺	0+2, 0+2ⁿ	0.53	2.17		0.50
2	2.94	2⁺	0, 0+2ⁿ	1.01	>5.86		0.62
3	3.58	0	2[i]	0.07	1.6		0.6
4	3.94	(3)⁺	0, 0+2ⁿ	1.56	4.54	1.78	0.61
5	4.32		~0.30[g]				
6	4.33	2⁺	}0, 0+2ⁿ ~0.29[g]	1.19	5.60	1.68	0.54
7	4.35		~0.60[g]				
8	4.83		(1,0)[ik]	0.33	5.54	2.46	0.79
9	4.90		2[ik]	0.47	1.41	0.87	0.19
10	4.97			0.01			
11	5.29		2[i]	1.05	1.01	1.08	0.21
12	5.47		2	0.65	1.31	0.94	0.27
13	5.69		~0.04[g]				
14	5.71		2 ~0.33[g] }0.37	1.12	0.82	0.52
15	6.12	(2,3)⁺	0, (0+2)[i]	1.76	3.50	1.45	0.44
16	6.25	(2,3)⁺	0	0.05			
17	6.62		2, (2+0)[i]	0.15	2.34	1.67	0.56
18	6.74		(0), (2+0)[i]	0.24	2.36	1.32	0.14
19	6.87		1	1.73	3.26	2.54	0.53
20	6.97			0.09			
21	7.06			$O_0{}^{17}$			
22	7.10						
23	7.24		small[g]				
24	7.25	}1 ~1.8[g] }4.13	>1.69	>2.47	0.51
25	7.27		~2.3[g]				
26	7.34	1	~0.8[g]				
27	7.35		small[g] }1.25	>6.45	4.34	0.40
28	7.38		~0.4[g]				
29	7.41						
30	7.53	1	0.39	7.5	4.6	0.6
31	7.67	}2 ~1.32[g] }1.32	1.44	1.54	0.18
32	7.68		~0.0[g]				
33	7.71	(2)	0.22	3.0	2.1	0.6
34	7.76		0.26	2.1	1.7	0.2
35	7.81	(1)[i]	0.74	4.51	2.5	0.73
36	7.83			...			
37	7.94		2.18[l]	0.90	0.94	0.52
38	8.02		0.11	9.5	1.7	2.6
39	8.04			...			
40	8.17	}(1)	0.52	3.84	4.21	0.77
41	(8.19)						
42	8.24	(0), 0[i]	1.27	>6.43	3.69	0.75
43	8.39		0.01			
44	8.45		0.17	3.5	1.2	0.5
45	8.49		~0.25[g] }0.53	2.78	1.81	0.28
46	8.52		~0.28[g]				
47	8.57			...			
48	8.62		0.20	0.9	0.5	0.5
49	8.66			...			
50	8.69	8.69[i]	0.62	2.71	2.16	0.41
51	8.85			...			

TABLE I (continued)

(1)	(2)		(3)	(4)	(5)	(6)	(7)
Group number[a]	Energy level[b] (MeV)		l[b]	$d\sigma/d\Omega(25°)$[c] (mb/sr)	$\frac{d\sigma}{d\Omega}$ relative[i] to $\frac{d\sigma}{d\Omega}(25°)$ 10°	15°	40°
	Mg²⁶				Mg²⁵(d,p)Mg²⁶		
52	8.89	8.90[i]		⎫ 0.87	5.71	3.56	0.58
53	8.92	8.91[i]		⎬			
54	8.95	8.94[i]		0.04			
55	9.03	⎫ 9.04[i]	(0)[i]	0.57	7.25	3.48	0.97
56	9.05	⎬					
57	9.10	9.10[i]		0.01			
58	9.16	9.15[i]		1.92	0.96	1.07	0.47
59	9.22	⎫ 9.24[i]		0.84	1.92	1.76	0.37
60	9.25	⎬					
61	9.30	9.31[i]		0.45	5.58	4.04	0.62
62	9.37	9.36[i]	(0)[i]	0.23	8.4	3.4	0.5
63	9.42	9.42[i]	(0)[i]	0.30	7.5	4.7	0.5
64	9.46	9.46[i]		0.27	2.6	1.8	0.1
65	9.53	⎫ 9.56[i]		1.83	3.52	3.04	0.40
66	9.56	⎬					
67	9.62	9.62[i]		0.03			
68	9.67	9.67[i]		0.05			
69	9.71	9.71[i]		0.23	3.3	2.0	
70	9.76	9.76[i]		0.16	1.8	0.9	
71	9.81	9.78[i]		0.02			
72	9.84	9.85[i]		0.23	3.7	2.8	
73	9.90	9.90[i]		0.12	1.4	1.1	
74	9.93	9.91[i]		0.07	3.2	2.0	
75	9.97	9.96[i]		0.27	2.5	⎫ 1.5	
76	10.03	10.03[i]		0.13	1.0	⎬	
77	10.09	10.09[i]		0.13	⎫ 3.46	3.05	
78	10.12	10.12[i]		0.71	⎬		
79	10.21	10.21[i]		0.23	1.65	1.54	
80	10.27			0.08			
81	10.32	10.31[i]		0.20	1.1	1.1	
82	10.36	10.35[i]		0.84	5.2	3.4	
83	10.40	⎫ 10.41[i]		0.03			
84	10.42	⎬					
85	10.48			0.02			
86	10.52			0.19	H	2.4	
87		10.59[i]		0.56	H	3.32	
88		10.64[i]		0.84	H	1.43	
89[h]		10.70[i]		1.63	H	1.54	
90[h]		10.91[i]		0.34	2.1	H	
91		10.98[i]		⎫ 0.53	1.4	H	
92		11.00[i]		⎬			
93		11.07[i]		0.75	2.86	H	
94	11.12 (3⁺)	⎫ 11.16[i]		0.89	2.2	2.1	
95	11.17 2⁺	⎬					
96	11.20 2⁺						
97		11.22[i]		0.06	5.9	3.3	
98		11.28[i]		0.41	1.8	1.3	
99		11.31[i]		0.34	1.6	⎫ 1.4	
100	(11.35)	11.34[i]		0.13	4.1	⎬	
101		11.38[i]		0.39	1.8	1.4	
102		11.45[i]		0.39	2.1	2.0	
103		11.48[i]		0.30	⎫ 1.8	1.5	
104		11.51[i]		0.62	⎬		
105		11.57[i]		0.22	2.3	2.1	
106		11.60[i]		0.11	1.8	1.8	
107		11.69[i]		0.71	2.5	1.7	
108		11.76[i]		0.22	⎫ 1.7	2.0	
109		11.79[i]		0.62	⎬	0.8	
110		11.83[i]		0.50	2.9	2.9	
111		11.90[i]		0.71	1.4	1.5	
112		12.00[i]		0.32	1.3	1.4	
113		12.50[i]		1.40	2.4	2.2	
114		12.57[i]		0.55	1.7	1.4	
	Mg²⁷				Mg²⁶(d,p)Mg²⁷		
0	0	1/2⁺	0	2.02	>7.7	3.84	1.06
1	0.984	(3/2)⁺⁺ⁱ	2	4.10	1.26	1.20	0.22
2	1.69	(3/2)⁺⁺ⁱ	2	2.00[e]	1.30	1.15	0.37
3	1.94			0.08	∼3.3	∼3.3	∼0.8
4	3.11			0.02	∼2.0	∼1.0	
5	3.42			0.08	∼0.2	∼0.2	

TABLE I (continued)

(1) Group number[a]	(2) Energy level[b] (MeV)		(3) l[b]	(4) $d\sigma/d\Omega(25°)$[c] (mb/sr)		(5) $\frac{d\sigma}{d\Omega}$ relative[i] to $\frac{d\sigma}{d\Omega}$ (25°) — 10°	(6) 15°	(7) 40°
	Mg^{27}					Mg$^{26}(d,p)$Mg^{27}		
6	3.47	1/2^{+i}	}0, (0+2)^i	~1.41^g		>3.6	2.74	0.79
7	3.48	(5/2$^+$)^i		~0.59^g	2.00			
8	3.56	(3/2)$^{-i}$	1		6.49	>2.6	>1.0	0.53
9	3.76	}(3/2$^+$)^i, (7/2$^-$)^i	2, (2+3)^i	~5.76^g				
10	3.78			~5.19^g	10.95	0.89	1.13	0.54
11	3.88				0.04			
12	4.15		(2)		0.59	2.00	1.80	0.33
13	4.39				0.03			
14	4.55	(5/2$^+$)^i			0.29	1.3	1.2	
15	4.76				0.02			
16	4.82	(1/2)$^{-i}$	1		2.53^e	6.10	3.64	
17	4.98				0.06			
18	5.02		1		0.12	5.9	1.6	
19	(5.17)				0.04			
20	5.29				0.02			
21	5.37				0.18	0.7		
22	5.41				0.22	1.3	1.1	
23	5.62		(2,3)^i		3.21^m	2.29	1.94	
24	5.74				}0.30	1.1	1.2	
25	5.76					1.2	1.2	
26	5.82				0.55	1.2	1.2	
27	5.92				0.27	...	2.5	
28	6.01				...			
29	6.07		(2,3)^i		2.66	2.13	1.92	
30	6.12				0.05			
31	6.15				0.04			
32	6.31				}0.04			
33	6.33							
34	6.50				0.06			
35	6.64				0.15	3.3	2.3	
36^h	6.71	1/2$^-$, Γ>75 keV			1.05	4.1	2.3	
37	6.81				0.25	0.8	0.7	
38	6.85	6.84^i			0.79	1.7	1.3	
39	6.91							
40	6.98	}6.99^i			2.50	3.91	2.25	
41	7.01							
42	7.03							
43		7.13^i			4.35	1.68	1.36	
44		7.21^i			0.53	2.1	1.6	
45		7.37^i			0.45	2.1	1.9	
46^h		7.47^i			4.45^j			
47^h		7.68^i			2.65^j			
48^h		7.77^i			0.88^j			
49		7.82^i			0.47	3.0	2.3	
50		7.95^i			0.49	2.0	0.9	
51		7.96^i			0.11	5.4	3.9	
52		7.99^i			0.15	3.9	2.8	
53		8.05^i			0.18	3.0	1.9	
54		8.08^i			0.10	~2.2	...	
55		8.19^i			0.15	~5.4	~2.8	
56		8.25^i			0.58	3.6	1.9	
57		8.37^i			0.58	3.4	1.6	
58		8.50^i			3.00	1.84	1.59	
59		8.62^i			1.93	2.51	2.00	
60		8.80^i			1.70	3.24	2.25	
61		8.94^i			0.64	2.1	1.8	

a Numbering is the same as in Ref. 1 up to 49, 41, and 42 within Mg^{25}, Mg^{26}, and Mg^{27}, respectively.
b Data are taken from Ref. 2 unless specified.
c Present work: cross section in center-of-mass system. The errors are about 10 to 20%.
d Data from Ref. 4; points mean that no assignment of l value was possible to the measured angular distribution.
e The proton group from C$^{12}(d,p)$C^{13} has been subtracted. Both groups are well separated at $\theta=10°$ and $\theta=15°$. As the angular distribution for C$^{12}(d,p)$C^{13} is known [J. N. McGruer, E. K. Warburton, and R. S. Bender, Phys. Rev. 100, 235 1956; E. W. Hamberger, ibid. 123, 619 (1961).], the subtraction could be well performed.
f See Ref. 3.
g The corresponding peaks were resolved in Ref. 1. The individual cross sections were estimated assuming the intensity ratio obtained from Ref. 1. This is only an approximation because the angle of observation as well as the incident deuteron energy are different.
h A level essentially broader than experimental resolution, or group of unresolved levels.
i Present work.
j The cross section quoted is at $\theta=15°$. At $\theta=25°$ the observation is inhibited by H$^1(d,p)$H^2 peak.
k Mostly.
l The proton group from O$^{16}(d,p)$O^{17} has been subtracted considering the magnitude of O$_0^{17}$ peak and the ratio of O$_1^{17}$ to O$_0^{17}$ peaks with Mg^{26} target, all at $\theta=25°$.
m The proton group from C$^{12}(d,p)$C^{13} has been subtracted considering the magnitude of C$_3^{13}$ peak at $\theta=15°$ and the ratio of C$_3^{13}$ peaks at 25° and 15° with Mg^{24} target.
n See Ref. 7.

TABLE II. Parameters[a] of the optical model potential $V = V_{Coul} - (V + iW)[1 - \exp(r - R)/a]^{-1}$ used in DWBA analysis of $Mg^{24}(d,p)Mg^{25}$ reaction.

Ref.	Mg25 state	Deuteron					Proton						Neutron			
		E_d	V	W	r_0	a	V	W	r_0	a	r_0'	a'	V^b	W	r_0	a
c	all	15	50d	16d	1.5d	0.59d	45e	40e	1.25e	0.65e	1.25e	0.47e	B_n	0	1.25	0.65
f	ground state	15	60	7	1.4	0.7	47	2	1.25	0.5			$= V_d$	0	1.4	0.7
f	0.58 MeV	10	96	12.3	1.4	0.7	50	4	1.25	0.5						
g	0.58 MeV	10	70	15	1.5	0.6	42	5	1.3	0.6			B_n, 45h	0	1.3	0.7

a In units of MeV and fermis.
b B_n means that the potential V was adjusted by a variational iteration procedure so as to give the correct binding energy and quantum state for the bound neutron.
c Present work.
d These values were obtained from elastic scattering analysis of 15.9-MeV deuterons by Melkanoff, Sawada, and Cindro [M. A. Melkanoff, T. Sawada, and N. Cindro, Phys. Letters 2, 98 (1962)].
e In this case the potential has the usual volume absorption only for real part, and it has a surface absorption for the imaginary part, to which the parameters r_0' and a' refer. Values for parameters were obtained from R. C. Johnson (private communication).
f Smith and Ivash (Ref. 22).
g Buck and Hodgson (Ref. 21).
h This value is the result of the variational iteration procedure mentioned in remark (b).

It is interesting to compare the various calculations with each other and with experimental data. Both the present and Smith and Ivash calculations fit the experi-
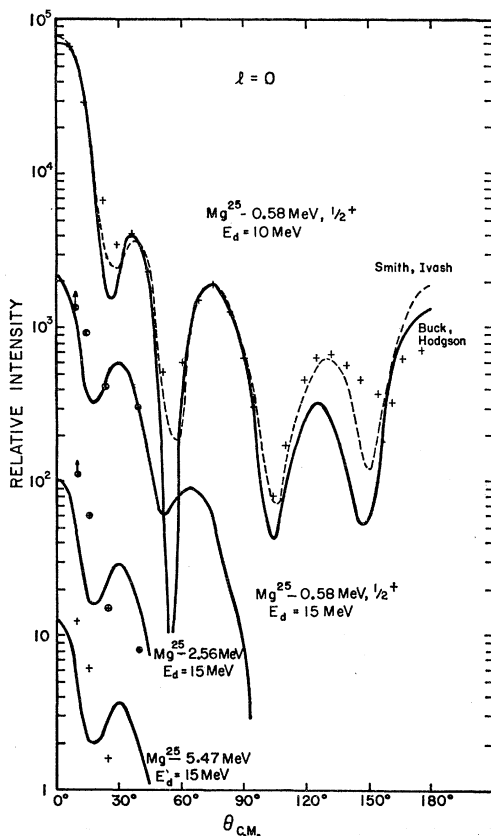

FIG. 4. Experimental and theoretical angular distributions for angular momentum transfer $l=0$. The curves are displaced arbitrarily along the vertical direction. The angular distributions are labeled by the residual nucleus and by the deuteron energy E_d. For comparison also the results for $E_d = 10$ MeV are reproduced; the experimental data are of Middleton and Hinds (Ref. 4), the theoretical of Buck and Hodgson (Ref. 19) and of Smith and Ivash (Ref. 20). The data for $E_d = 15$ MeV are from present work. The arrow attached to some points at $\theta_{c.m.} = 10°$ indicates that the point represents a lower limit only. The theoretical curves are calculated in DWBA method with parameters given in Table II and $B_n = 6.75$ MeV and $Q = 4.52$ MeV.

mental angular distribution for Mg^{25} ground state ($l=2$) and $E_d = 15$ MeV very well (Fig. 5). Both curves are essentially the same from 0° to 60°; at larger angles the Smith and Ivash calculations give larger cross sections, due to the smaller value of W (Table II). Unfortunately, the angular distribution has not been measured at backward angles; the two points at 70° and 93° suggest, however, an even smaller cross section than is predicted by the present calculation. It is surprising that neither Smith and Ivash nor Buck and Hodgson could fit the angular distribution for the same reaction (Mg^{25} ground state) initiated with $E_d = 10$ MeV. On the other hand, they both got a good fit for the Mg^{25} first excited state ($l=0$, initiated with $E_d = 10$ MeV) (Fig. 4), while the present calculation for $E_d = 15$ MeV gives a poor fit to the four experimental points. In general, the present calculations fit very well the experimental points in the cases of $l=2$, $l=1$, and $l=3$, but not in the case of $l=0$. This is evident from Figs. 4 to 7, which represent the calculated and experimental angular distributions for cases when the spin of the final state is known. The experimental angular distributions for $l=0$ and $l=1$ are in fact so similar that they cannot be distinguished from one another, on the basis of the only four points measured. On the other hand, the distinction is possible between $l=2$ and $l=3$ transitions for low excitation energies ($E < \sim 5$ MeV). In general, on the basis of only four or three points measured it is easy to decide only between the two possibilities $l=0$ or 1 and $l=2$ or 3. Moreover, when the excitation energy gets close to the neutron separation energy, no definite conclusion is possible.

The absolute value of the calculated cross sections can be checked only if the absolute value of the experimental cross section has been measured, and if the spectroscopic factor is safely predicted by the theory. This is the case, e.g., for the $Mg^{24}(d,p)Mg^{25}$ ground state ($l=2$) with $E_d = 15$ MeV. The ratio of experimental to calculated cross section is 0.10 with Smith and Ivash calculation, and it is 2.26 with the present calculation. As the theoretical value is 2 (see next section), the present calculation predicts the absolute value for cross
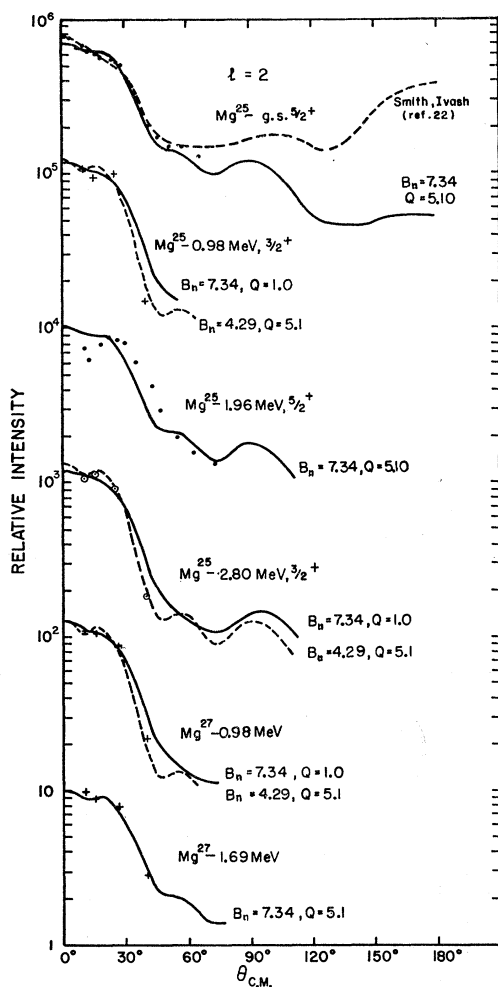
FIG. 5. Experimental and theoretical angular distributions for angular momentum transfer $l=2$ and deuteron energy $E_d=15$ MeV. The curves are displaced arbitrarily along the vertical direction. The angular distributions are labeled by the residual nucleus. The curves calculated in the present work, are labeled by B_n and Q values, used in computation; the values of other parameters used are given in Table II. The experimental angular distributions for Mg^{25}-ground state and Mg^{25}-1.96 MeV are from Hamburger and Blair (Ref. 21).

the corrections for different binding energies of captured neutron and for different energies of outgoing protons are more important. Finally, it is not clear what value should be used for binding energy, B_n of the captured neutron: the binding energy of the single-particle level in spherical potential well (which is the same for all levels with a certain l_j), or the binding energy of Nilsson level, or simply the binding energy of the actual (perturbed) state. In the last case the binding energy is simply related to the reaction Q value:

$$B_n = Q + 2.225 \text{ MeV}. \tag{1}$$

To retain some flexibility, the calculations were performed for independent sets of both Q and B_n values, chosen in the region of physically meaningful values (Table III). The cross section for any other value of Q' and B_n' is well obtained by interpolation formula

$$d\sigma(Q',B_n')/d\Omega = (d\sigma(Q,B_n)/d\Omega) A^{Q'-Q} B^{-B_n'+B_n}. \tag{2}$$

Assuming relation (1), relation (2) may be written

$$d\sigma(Q')/d\Omega = (d\sigma(Q)/d\Omega)(A/B)^{Q'-Q}. \tag{3}$$

The interpolation parameters A and B were obtained at $\theta = 25°$ for individual values of l and are represented in Table III.

INTERPRETATION OF LOW-LYING STATES OF Mg^{25}, Mg^{26}, AND Mg^{27} IN TERMS OF ROTATIONAL MODEL

A. Theory

It is well known[2] that the low-lying states of Mg^{24} nucleus[8] and of Mg^{25} nucleus[9] are very pure rotational

section very well, while the cross section calculated by Smith and Ivash is too large by a factor of 20.

As the last case shows, the present DWBA calculations could be applied with success also to light nuclei, such as magnesium. However, they have to be applied with caution. In addition to some disagreements between theory and experiment, which have been mentioned, certain difficulties that have not been met with heavy and medium weight nuclei are anticipated *a priori*. First, the nuclei in magnesium region are known to be deformed, while DWBA calculation considers strictly spherical symmetry. Secondly, the levels of the same l_j value of the stripped neutron are spread over an interval of about 8 MeV, in contrast to about 2 MeV with heavy and medium weight nuclei, and consequently
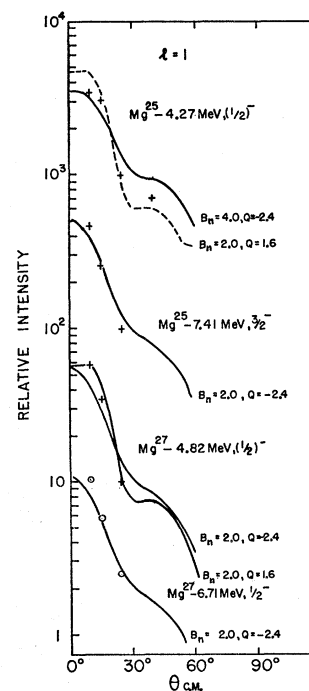
FIG. 6. Experimental and theoretical angular distributions for angular momentum transfer $l=1$ and deuteron energy $E_d=15$ MeV. The curves are displaced arbitrarily along the vertical direction. The angular distributions are labeled by the residual nucleus, and the calculated curves by B_n and Q values (in MeV) used in computation.

Table III. Calculated single-particle cross sections and interpolation parameters.[a]

l	Q[b]	B_n	$d\sigma/d\Omega(25°)$ mb/sr	$d\sigma/d\Omega$ relative to $d\sigma/d\Omega(25°)$ 10°	15°	40°	A	B	A/B
0	4.52[c]	6.75[c]	5.1	1.59	0.66	0.58	1.15	1.11	1.04
	4.52	8.50	4.5	1.16	0.51	0.60			
	1.00	8.50	2.7	1.18	0.89	0.63			
2	5.10[c]	7.34[c]	1.8	1.13	1.13	0.37	1.03	1.22	0.85
	5.10	4.29	3.7	1.22	1.32	0.22			
	1.00	7.34	1.5	1.31	1.28	0.33			
1	1.6	2.0	5.8	5.17	3.96	0.69	1.24	1.21	1.02
	−2.4	2.0	2.6	3.08	2.19	0.61			
	−2.4	4.0	1.9	2.58	2.10	0.76			
	−6.4	2.0	1.1	1.50	1.35	0.58			
3	1.6[c]	4.0[c]	1.3	0.77	0.85	0.63	1.03	1.40	0.74
	1.6	2.0	2.5	0.83	0.91	0.48			
	−2.4	2.0	1.7	1.13	1.13	0.49			
	−6.4	2.0	0.8	1.25	1.24	0.59			

[a] Interpolation parameters A, B, and A/B refer to Eqs. (2) and (3) in text. The numerical values are for $d\sigma/d\Omega(25°)$.
[b] Q is related to the excitation energy of the final nucleus as $Q = Q_0 - E^*$, where $Q_0 = 5.10$ MeV for $Mg^{24}(d,p)Mg^{25}$, $Q_0 = 4.21$ for $Mg^{26}(d,p)Mg^{27}$, and $Q_0 = 8.89$ MeV for $Mg^{25}(d,p)Mg^{26}$.
[c] The relation $B_n = Q + 2.23$ is (approximately) fulfilled.

states. In the following we shall discuss to what extent the low-lying states of Mg^{26} and Mg^{27} may also be interpreted as rotational states. In the case of Mg^{27} we shall do this by comparing the $Mg^{26}(d,p)Mg^{27}$ cross sections with theoretical predictions and with $Mg^{24}(d,p)$-Mg^{25} experimental cross sections. In the case of Mg^{26} we have at our disposal only the comparison of $Mg^{25}(d,p)Mg^{26}$ experimental cross sections with theoretical predictions, for there are no corresponding $Mg^{23}(d,p)Mg^{24}$ experiments.

In the rotational model, the wave function of the nucleus is expressed as a product of a function ϕ, describing the vibration of the nucleus, of the function $D_{KM}{}^I(\alpha\beta\gamma)$, describing the rotation of the nucleus, and of the function X_Ω, describing the internal motion of the
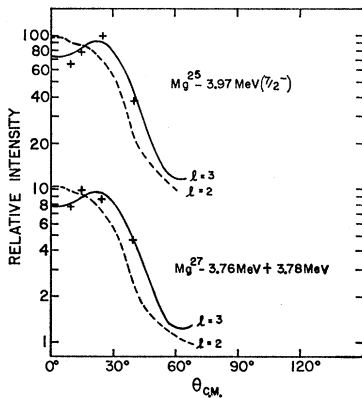

FIG. 7. Experimental angular distributions for Mg^{25}-3.97-MeV levels and Mg^{27}-3.76-MeV+3.78-MeV levels, with theoretical curves for angular momentum transfer $l=3$ ($B_n=2.0$ MeV, $Q=1.6$ MeV) and $l=2$ ($B_n=7.34$ MeV, $Q=1.0$ MeV). Only the $l=3$ curves fit the experimental points. Both curves are displaced arbitrarily along the vertical direction.

nucleus in a deformed, axially symmetric potential:

$$\psi(IMK\Omega) = \left(\frac{2I+1}{16\pi^2}\right)^{1/2}$$

$$\times \phi\{X_\Omega D_{KM}{}^I + (-)^{I-J}X_{-\Omega}D_{-KM}{}^I\}. \quad (4)$$

The internal wave function X_Ω is the antisymmetrized product of single-particle wave functions $X_{\Omega\omega\alpha}$, for which the projection of angular momentum j on symmetry axis (Ω), the parity (ω), and the energy (α) are good quantum numbers.

According to Nilsson,[13] the functions $X_{\Omega\omega\alpha}$ are the solutions to the Hamiltonian

$$H = H_0 + C\mathbf{l}\cdot\mathbf{s} + D\mathbf{l}^2, \quad (5a)$$

with

$$H_0 = \tfrac{1}{2}\hbar\omega_0(-\Delta+r^2) - \delta\hbar\omega_0\tfrac{4}{3}(\pi/3)^{1/2}r^2Y_{20}. \quad (5b)$$

The deformation of the potential well is expressed here with the parameter δ, but more often it is given in terms of the parameter η, which is related to δ as:

$$\eta = -\frac{\delta}{\kappa}\frac{\omega_0}{\omega_0{}^0} = \frac{\delta}{\kappa}\left(1-\frac{4}{3}\delta^2-\frac{16}{27}\delta^3\right)^{-1/6}, \quad (5c)$$

where $\kappa = \tfrac{1}{2}(C/\hbar\omega_0{}^0)$, and $\omega_0{}^0=\omega_0(\delta=0)$. The numerical value for κ, adopted by Nilsson, is 0.05.

The functions $X_{\Omega\omega\alpha}$ are expressible with wave functions of spherically symmetric potential, $\phi_{Nlj\Omega}$:

$$X_{\Omega\omega\alpha} = \sum_{Nlj} c_{Nlj}(\Omega\omega\alpha)\phi_{Nlj\Omega}. \quad (6)$$

The summation above refers actually only to different orbitals l, j of the same shell ($N=$const), since the model neglects the interaction between different shells.

The coefficients $c_{Nlj}(\Omega\omega\alpha)$ are related to coefficients $a_{Nl\Lambda}$, tabulated by Nilsson[13] as:

$$c_{Nlj}(\Omega\omega\alpha) = \sum_\Lambda a_{Nl\Lambda}\langle l\tfrac{1}{2}\Lambda l \,|\, j\Omega\rangle.$$

They have been calculated for the region of interest for deformation parameters $\eta=2$ and $\eta=4$, following Nilsson,[13] and, in addition, for the $N=2$ shell, following Bishop,[22] too (Table IV). Bishop adopted for the parameter $\mu=2D/C$ the value $\mu=0.33$, while Nilsson took $\mu=0$. With this choice of parameter μ, Bishop causes the orbit $5/2(+)5$ to remain below orbit $1/2(+)9$ when $\eta\lesssim3.6$, while with Nilsson this is the case only when $\eta<2.9$. The coefficients $c_{Nlj}^2(\Omega\omega\alpha)$ obey the following two sum rules:

$$\sum_{\substack{Nlj\\ \Omega\omega\alpha=\text{const}}} c_{Nlj}^2(\Omega\omega\alpha)=1 \tag{7}$$

and

$$\sum_{\substack{\Omega\omega\alpha\\ Nlj=\text{const}}} c_{Nlj}^2(\Omega\omega\alpha)=2j+1. \tag{8}$$

In (7) the summation refers to all orbits lj of a particular state N that contribute to a certain level $\Omega\omega\alpha$, while in (8) it refers to all levels $\Omega\omega\alpha$ that receive some contribution from a given unperturbed orbit Nlj.

As derived by Satchler,[12] the spectroscopic factor S, expressing the overlap between initial and final nucleus of a stripping reaction, is

$$S=g^2\frac{2I_i+1}{2I_f+1}\langle I_ijK_i\Omega\,|\,I_fK_f\rangle^2\langle\phi_f\,|\,\phi_i\rangle^2 c_{Nlj}^2(\Omega\omega\alpha), \tag{9}$$

where the quantities with subscript i refer to the initial nucleus, those with subscript f to the final nucleus, and

TABLE IV. Values[a] for $c_{Nlj}^2(\Omega\omega\alpha)$ in dependence on deformation parameter η.

$\Omega\omega\alpha$	N	l	j	Nilsson[b]			Bishop[b]	
				$\eta=2$	$\eta=4$	$\eta=6$	$\eta=2$	$\eta=4$
1/2(+)6	2	0	1/2	0.157	0.246			
	2	2	3/2	0.017	0.058			
	2	2	5/2	0.825	0.699			
3/2(+)7	2	2	3/2	0.016	0.041			
	2	2	5/2	0.985	0.960			
5/2(+)5	2	2	5/2	1	1	1	1	1
1/2(+)9	2	0	1/2	0.651	0.280	0.137	0.668	0.177
	2	2	3/2	0.179	0.458	0.569	0.334	0.653
	2	2	5/2	0.171	0.260	0.295	0.000	0.163
1/2(+)11	2	0	1/2	0.195	0.474	0.579	0.592	0.650
	2	2	3/2	0.805	0.486	0.340	0.363	0.290
	2	2	5/2	0.004	0.044	0.084	0.043	0.055
3/2(+)8	2	2	3/2	0.985	0.964			
	2	2	5/2	0.015	0.041			
1/2(−)14	3	1	1/2	0.104	0.012			
	3	1	3/2	0.312	0.425			
	3	3	5/2	0.160	0.138			
	3	3	7/2	0.425	0.425			

[a] The list is complete only for $N=2$ (d-s shell).
[b] Bishop (Ref. 22) uses for parameter $\mu=2D/C$, related to Hamiltonian Eq. (5a), the value of 0.33, while Nilsson (Ref. 13) uses with $N=0, 1, 2$, $\mu=0$, and with $N=3$, $\mu=0.35$.
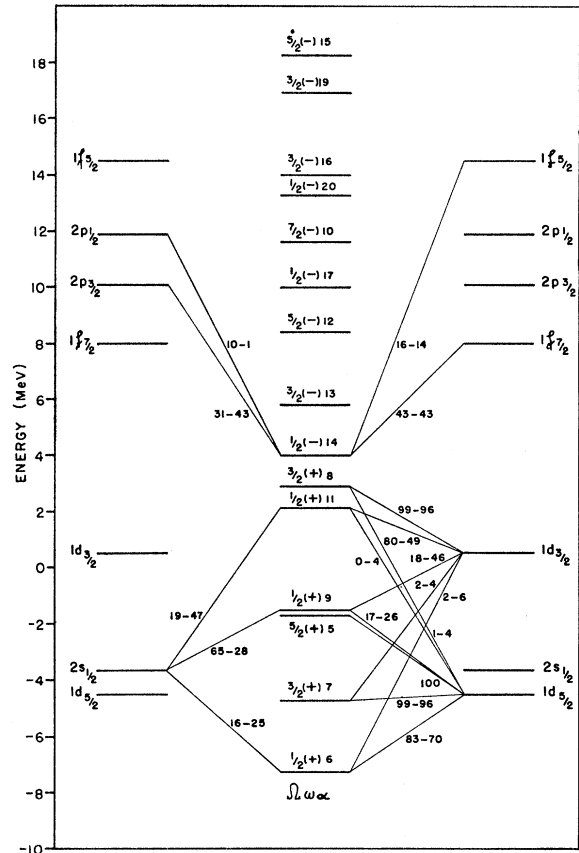
[22] G. R. Bishop, Nucl. Phys. 14, 376 (1959/60).

FIG. 8. Single-particle energy levels $(\Omega\omega\alpha)$ of an axially symmetric potential well with deformation parameter $\eta=3.6$. These are essentially Nilsson levels (Ref. 13) except for d-s shell, where the Bishop (Ref. 22) calculations with $\mu=0.33$ were adopted, giving the correct sequence of levels $5/2(+)5$ and $1/2(+)9$. The single-particle energy levels of spherically symmetric potential well (Nlj) are also shown, and the numerical values (in percent) for coefficients $c_{Nlj}^2(\Omega\omega\alpha)$ are given for deformation parameters $\eta=2$ and $\eta=4$.

those without subscript to the transferred neutron. The coefficient $g^2=2$ if either $K_i=0$ or $K_f=0$, and $g^2=1$ otherwise.

The experimental (d,p) cross section is related to the calculated single-particle cross section as

$$d\sigma(\theta)/d\Omega=\frac{2I_f+1}{2I_i+1}S(d\sigma(\theta)/d\Omega)_{\text{sp}}. \tag{10}$$

In the case that more than one value of l and j contribute to a transition to a certain final state, this relation may be replaced under certain conditions (neglecting spin-orbit term of optical potential) by

$$d\sigma(\theta)/d\Omega=\frac{2I_f+1}{2I_i+1}\sum_{lj} S_{lj}(d\sigma_{lj}(\theta)/d\Omega)_{\text{sp}}. \tag{11}$$

In the case that the target is an even-even nucleus with $I_i=K_i=0$, only one value of j, $j=I_f$, occurs in a
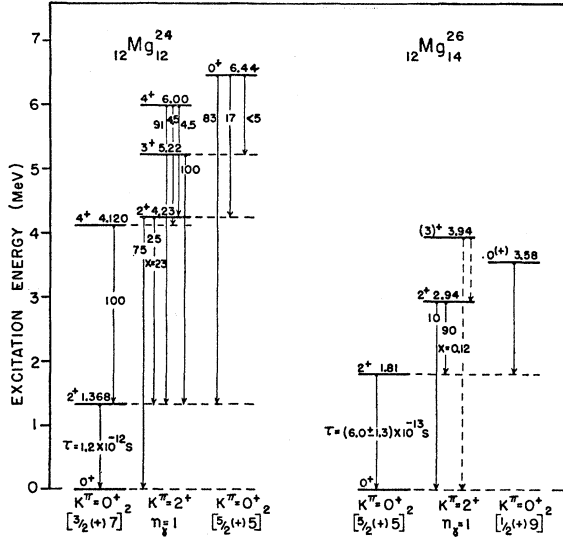
FIG. 9. Established and proposed rotational bands for Mg²⁴ and Mg²⁶, respectively. The observed gamma-ray transitions are also shown; x gives the ratio of $E2$ to $M1$ amplitude. Each band is characterized by the quantum number K, indicating the projection of the spin on the symmetry axis, and by parity. Moreover, for the bands with a simple single-particle configuration, this is given for the last two neutrons in terms of quantum numbers $\Omega\omega\alpha$. The one-phonon vibrational band is marked by the number of phonons: $n_\gamma=1$. Each level is marked by the value of its spin and energy (in MeV).

certain transition, and $\Omega=K_f$. The Clebsh-Gordan coefficient in Eq. (9) equals unity, and for most cases $\langle\phi_f|\phi_i\rangle^2=1$, because in general the vibration of the nucleus does not change. Thus the equation (9) simplifies to

$$S=2c_{Nlj}{}^2(\Omega\omega\alpha)/(2j+1) \qquad (12)$$

and the cross section is simply

$$d\sigma(\theta)/d\Omega=(2j+1)S(d\sigma(\theta)/d\Omega)_{\rm sp}$$
$$=2c_{Nlj}{}^2(\Omega\omega\alpha)(d\sigma(\theta)/d\Omega)_{\rm sp}. \qquad (13)$$

In the case that the target is an even-odd nucleus with spin I_i, K_i, in general more values of l and j contribute to the transition to a final state with spin I_f, K_f. There is, however, an additional selection rule for j values, arising from the rotational model condition: $j\geq|\Omega|$ $=|K_f-K_i|$. Thus, e.g., for the Mg²⁵(d,p)Mg²⁶ transition to the first excited state, we have $I_i=K_i=5/2^+$ and $I_f=2^+$. If the first state belongs together with the ground state to the rotational band $K_f=0$, Ω of the transferred neutron $\Omega=|K_f-K_i|=5/2$; thus only $j=5/2$, $l=2$ is allowed, although the conservation of spins makes possible also the contribution of $j=1/2$, $l=0$. Furthermore, the ratio of spectroscopic factors for transitions to two levels of the same rotational band is

$$\frac{S(I_f{}')}{S(I_f)}=\frac{2I_f+1}{2I_f{}'+1}\frac{\langle I_i jK_i\Omega|I_f{}'K_f\rangle^2}{\langle I_i jK_i\Omega|I_fK_f\rangle^2}, \qquad (14)$$

what follows from Eq. (9), since g^2, $\langle\phi_f|\phi_i\rangle^2$, and $c_{Nlj}{}^2(\Omega\omega\alpha)$ are the same in both cases.

B. Comparison Between Experimental and Theoretical Results

Mg²⁵ Nucleus

All 14 states up to 4.27 MeV have already been[3,9] identified as members of four rotational bands. In Table VI we compare the so-called experimental values for $c_{Nlj}{}^2(\Omega\omega\alpha)$, obtained according to Eq. (13) from experimental cross sections and single particle cross sections calculated in DWBA, with the theoretical values calculated for the Nilsson Hamiltonian (5) with deformation parameter $\eta=4$. This particular value for η is supported by the predicted equilibrium deformation and by the decoupling parameter, which is for $\eta=4$ in best agreement with experimental levels for the three $K=1/2$ bands. The agreement between experimental and theoretical values for $c_{Nlj}{}^2(\Omega\omega\alpha)$ is excellent (within 20%) with the bands 5/2(+)5 and 1/2(+)9, and is reasonably good with the bands 1/2(+)11 and 1/2(−)14. We must however be aware of the error in the calculated single-particle cross section (~20%) and of the fact that some of the theoretical $c_{Nlj}{}^2(\Omega\omega\alpha)$ are very sensitive to the changes in deformation (Table IV). There is, moreover, an additional ambiguity in single-particle cross sections regarding the binding energies B_n used in calculations. In the present evaluation the binding energies of the perturbed states $(B_n=Q+2.225$ MeV$)$ were adopted. The binding energies of the unperturbed single particle levels are essentially smaller with cases of the $1f_{7/2}$, $2p_{3/2}$, $1p_{1/2}$, and $1f_{5/2}$ levels, which are expected to be already in the continuum region $(B_n<0)$. The single-particle cross sections are increasing with decreasing binding energy. Therefore the experimental $c_{Nlj}{}^2(\Omega\omega\alpha)$ values for the 1/2(−)14 band would be smaller and in better agreement with theory if the binding energies of the unperturbed single-particle levels were used in the DWBA calculations. The discrepancy between experimental and theoretical values is, however, not larger than by a factor of four and may also be due to mixing between the bands 1/2(−)14, 3/2(+)13, and 5/2(−)12, caused by rotational particle coupling.

It is surprising that no level of band 3/2(+)8 has been identified, although the first level $(I=3/2)$ is expected to have a large (d,p) cross section (~4 mb/sr) and to be at about 4-MeV excitation energy.

Mg²⁶ Nucleus

We are limiting the present discussion to the first five states, for which some information about the spins and parities exist. Matching them with corresponding levels of Mg²⁴ we obtain an indication as to which rotational bands they might be ascribed (Fig. 9).

From this comparison, we immediately notice the following features:

(1) The second $K=0^+$ band is essentially lower in Mg²⁶ than in Mg²⁴. This is understandable by very plausible arguments. According to the Nilsson level

TABLE V. Experimental and theoretical results on low-lying levels of Mg²⁶.

Energy level (MeV)		Band	$d\sigma/d\Omega(25°)$ Experiment[a]		B_n[b]	$d\sigma/d\Omega(25°)_{sp}$		Experiment[c]			Theory[d]	
			$l=0$	$l=2$		$l=0$	$l=2$	$S(l=0)$	$S(l=2)$	$S(l=2)/S_g$	$S(l=2)$	$S(l=2)/S_g$
0	0⁺	$K^\pi=0$, $[5/2(+)5]^2$	···	0.44	9.23	···	1.39	···	1.90	1	2	1
1.81	2⁺		0.09	0.44	9.23	5.55	1.31	0.02	0.40	0.21	0.72	0.36
2.96	2⁺	$K=2^+$, $N_\gamma=1$	>0.70	<0.31	6.74	7.10	2.10	>0.12	<0.18	<0.09		
3.94	(3)⁺		0.77	0.79	6.74	6.22	2.02	0.11	0.34	0.18		
3.58	0	$K^\pi=0^+$, $[1/2(+)9]^2$	···	0.07	9.00	···	1.30	···	0.32	0.17	0	

ᵃ Obtained from experimental cross sections at 10° and 25° (Table I), considering that the ratio of these two cross sections is ∼8.0 for pure $l=0$ transition and ∼1.1 for pure $l=2$ transition.
ᵇ These are the neutron binding energies which were adopted in the calculation of the single-particle cross sections. They refer to Nilsson orbits. The binding energy of the lowest orbit 5/2(+)5 is taken as the mean value of the neutron separation energies of Mg²⁵ and Mg²⁶. The orbit 1/2(+)9 is only a little above orbit 5/2(+)5. To the one-phonon states the orbits 5/2(+)5, 1/2(+)9, 1/2(+)11, and 3/2(+)8 contribute; the mean binding energy is thus about 6.74 MeV.
ᶜ Obtained according Eq. (10).
ᵈ Obtained according Eq. (9).

scheme (Fig. 8), with the ground state $(K=0^+)$ configuration of Mg²⁴, all levels up to the level 3/2(+)7 inclusive are completely filled. To get the next $K=0^+$ configuration, two identical nucleons from the level 3/2(+)7 have to be elevated to the next, 5/2(+)9 level. Thus, the two $K=0^+$ bands are expected to be separated in energy by twice the separation energy between the levels 3/2(+)7 and 5/2(+)5, that is for about 6 MeV, which is actually the case. On the other hand, with the ground-state configuration of Mg²⁶, all neutron levels up to 5/2(+)5 are completely filled. To get the next $K=0^+$ configuration, the last two neutrons have to be elevated to the next, 1/2(+)9 level. The separation between the two $K=0^+$ bands is expected to be small because of the proximity of the 5/2(+)5 and 1/2(+)9 levels.

(2) The one-phonon vibrational band $K=2^+$, $N_\gamma=1$ is lower in Mg²⁶ than in Mg²⁴. The two $I=2^+$ levels, one from the $K=0^+$ and the other from the $K=2^+$ band, which are well separated in Mg²⁴, are only 1.13 MeV apart in Mg²⁶. The mixing between them, which practically does not occur in Mg²⁴, is expected to be important in the Mg²⁶ case.

(3) The separation between the ground and first excited state is somewhat larger in Mg²⁶ than in Mg²⁴. This may indicate a smaller deformation for Mg²⁶, but may also be a perturbation effect arising from interaction between the two $I=2^+$ states.

Let us now investigate how much the Mg²⁵(d,p)Mg²⁶ cross sections, together with other experimental data, confirm the level scheme proposed in Fig. 9.

$K=0^+$ band: ground state, 0^+ and 1.81-MeV 2^+ state

If the 1.81-MeV 2^+ state is a pure state of the rotational band $K=0^+$, only $l=2$ angular momentum transfer is allowed in the Mg²⁵(d,p)Mg²⁶ reaction, as discussed in the preceding section. Actually, the contribution of $l=0$ angular momentum is rather small, only 5% in spectroscopic factors (Table V). For the two states belonging to the same rotational band, the ratio S_2/S_g, predicted according to Eq. (14), amounts to 0.36, in satisfactory agreement with the experimental value

0.21. The ratio S_2/S_g for the same two Mg²⁶ states was measured[17] also with the Al²⁷(d,He^3)Mg²⁶ reaction; the experimental value 1.87, was again very close to the theoretical value, 1.78. Furthermore, the enhancement, characteristic for $E2$ transitions within the same rotational band, is present. The mean lifetime of the 1.81-MeV 2^+ state is $(6.0\pm1.3)\times10^{-13}$ sec, which is close to the lifetime derived from the corresponding transition in Mg²⁴ applying the energy correction $(3\times10^{-13}$ sec), and is essentially smaller than the $E2$ single particle value $(10^{-11}$ sec). Accordingly, the 1.81-MeV 2^+ state may be interpreted as the 2^+ rotational state of band $K=0^+$ with small admixtures $(\lesssim10\%)$ present.

$K=2^+$, $N_\gamma=1$ band: 2.94-MeV 2^+ and 3.94-MeV $(3)^+$ levels

According to recent understanding, the vibrational or so-called phonon state is nothing but a superposition of many two quasiparticle states. Formerly, it had been believed[12] that the vibrational states are only very weakly excited in stripping reactions. Subsequent experimental[23] and theoretical[24] work has shown however, that this is not true, and that the vibrational states in even-even final nuclei are in fact as strongly excited as the ground state.

Both $l=0$ and $l=2$ components of a transferred angular momentum are expected for transitions in question because of the complicated nature of the phonon state and because they are both allowed by selection rule $j\geq|\Omega|=|K_f-K_i|$, giving in the present case $j\geq1/2$. In fact, the states 2.94-MeV 2^+ and 3.94-MeV $(3)^+$ are quite strongly excited in the Mg²⁵(d,p)Mg²⁶ reaction; the contribution of $l=0$ is essentially larger than in the transition to the 1.81-MeV state of the $K=0^+$ rotational band. Accordingly, everything in the present experiment agrees with the idea that the 2.94- and 3.94-MeV levels are members of the $K=2^+$ vibrational band.

²³ B. L. Cohen and R. E. Price, Phys. Rev. 118, 1582 (1960).
²⁴ S. Yoshida, Nucl. Phys. 38, 380 (1962).

On the other hand, the observed[2] electromagnetic transition of the 2.94-MeV state shows that this state is not as pure a $K=2^+$ vibrational state as is the corresponding 4.23-MeV state of Mg^{24}. According to the rotational model selection rule, $L \geq \Delta K$, no $M1$ transition is allowed between $K=2^+$ and $K=0^+$ bands. Actually, while in the analogous transition 4.23 MeV, 2^+ to 1.367 MeV, 2^+ of Mg^{24}, the $E2$ component predominates (the ratio of $E2$ to $M1$ amplitude, $x=23$), the transition 2.94 MeV, 2^+ to 1.81 MeV, 2^+ of Mg^{26} contains more of $M1$ than of $E2$ component ($x=0.12$). The forbiddenness of the $M1$ transition may, however, be violated by the presence of only small admixtures in wave functions.

The observation of the transition 3.94 MeV, $(3)^+$ to 2.94 MeV, 2^+ together with the absence of the transition 3.94 MeV, $(3)^+$ to 1.81 MeV, 2^+ support the idea that
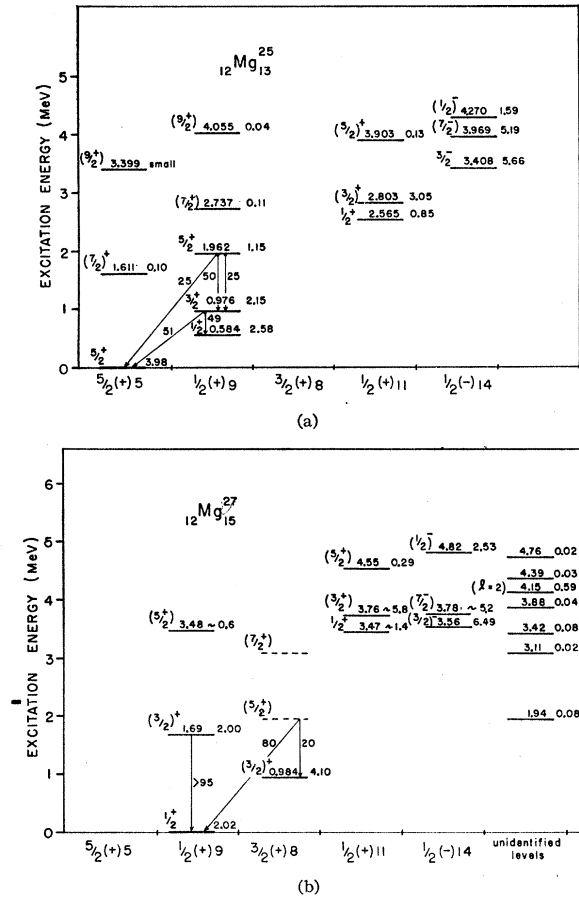

(a)

(b)

FIG. 10. Established and proposed rotational bands for Mg^{25} and Mg^{27}, respectively, with observed gamma-ray transitions. Each band is characterized by the single-particle configuration, given in terms of quantum numbers $\Omega \omega \alpha$ (see text) of the unpaired neutron. Each level is marked by the value of its spin, energy (in MeV), and stripping cross section (in mb/sr) for 15-MeV deuterons at $\theta_{c.m.}=25°$ (the number on the right).

Note: The numbers indicating the branching ratio of the 1.94-MeV $(5/2^+)$ level of Mg^{27} are by mistake interchanged. Correctly, the level decays 80% to the 0.984-MeV level and 20% to the ground state.

the 2.94 MeV, 2^+ and 3.94 MeV, $(3)^+$ states are members of the same rotational band.

$K=0^+$, 3.58 MeV, $I=0^{(+)}$ level

As discussed at the beginning of this section, we expect the second $K=0^+$ band to have the configuration $(5/2(+)5)^{-2}(1/2(+)9)^2$. As the Mg^{25} ground state is a very pure $(5/2(+)5)^1$ state, a state with the above-mentioned configuration of Mg^{26} cannot be excited in a $Mg^{25}(d,p)Mg^{26}$ reaction, unless some component of configuration $(5/2(+)5)^2$ is also present, i.e., unless the ground state and the 3.58-MeV state are mixed. The mixing is possible only between the states of the same spin and parity. Therefore we tentatively assume that the state at 3.58 MeV has positive parity. This mixing cannot be ascribed to rotation-particle coupling, since this occurs only between the states with $\Delta K=1$, but is due to the residual interaction.

If the wave functions of nuclei in question are written as

$$\psi(Mg_{gs}^{25}) = (5/2(+)5)^1, \tag{15a}$$

$$\psi(Mg_{gs}^{26}) = \alpha(5/2(+)5)^2 + \beta(1/2(+)9)^2, \tag{15b}$$

$$\psi(Mg_{3.58}^{26}) = -\beta(5/2(+)5)^2 + \alpha(1/2(+)9)^2, \tag{15c}$$

the spectroscopic factor for $Mg^{25}(d,p)Mg_{gs}^{26}$ transition is proportional to α^2, and the spectroscopic factor for $Mg^{25}(d,p)Mg^{26}$ 3.58-MeV transition is proportional to β^2. Thus, $S_{3.58}/S_g = \beta^2/\alpha^2$. Experimentally, we obtained $S_{3.58}/S_g = 0.17$. This same ratio β^2/α^2 may also be evaluated in the $Mg^{26}(d,t)Mg^{25}$ experiment, leading to the Mg^{25} ground state and 2.58 MeV, $1/2^+$ state. Here the ratio $S_{2.58}/S_g = \beta^2/\alpha^2$. Experimentally, the value $S_{2.58}/S_g = 0.16$ was obtained.[21] The fact that both different experiments give practically the same value for β^2/α^2 strongly supports our assumption concerning the parity and the configuration of the 3.58-MeV level of Mg^{26}.

Mg^{27} Nucleus

The experimental data about the levels of Mg^{27} are rather sparse. The spins of the levels are unknown except for the ground state ($I=1/2^+$) and the broad ($\Gamma > 75$ keV) level at 6.71 MeV ($I=1/2^-$). We know also that one of the levels at 3.47 or 3.48 MeV has $I=1/2^+$, because the (d,p) angular distribution for both levels combined is very close to $l=0$ in appearance. We assigned spin and parity $1/2^+$ to the 3.47-MeV level, which shows a larger (d,p) cross section than the 3.48-MeV level in the case[1] where both levels were resolved. For most other low-lying levels the l values of the transferred neutron are known, allowing for the spin two possibilities: $I=l\pm 1/2$.

A few gamma-ray transition data, represented in Fig. 10(b), were obtained recently by Becker et al.[25]

[25] J. A. Becker, G. E. Mitchell, and P. F. Donovan, Bull. Am. Phys. Soc. 8, 319 (1963).

TABLE VI. Paralleling of Mg^{27} low-lying levels with known rotational levels of Mg^{25} according to observed l values and (d,p) cross sections.

$\Omega\omega\alpha$, I^{π}	Energy level, I^{π}, l_n Mg^{25}	Mg^{27}	$d\sigma/d\Omega(25°)$ exptl. (mb/sr) Mg^{25}	Mg^{27}	$c_{Nlj}{}^2(\Omega\omega\alpha)$ exptl.[a] Mg^{25}	Mg^{27}	$c_{Nlj}{}^2(\Omega\omega\alpha)$ theory[b]
5/2(+)5, 5/2$^+$	g.s. 5/2$^+$ 2		3.98	...	1.10	...	1.00
7/2$^+$	1.611 (7/2$^+$) (4)		0.10	...	...	...	...
9/2$^+$	3.399 (9/2$^+$) (4)		small	...	...	...	...
1/2(+)9, 1/2$^+$	0.584 1/2$^+$ 0	g.s. 1/2$^+$ 0	2.58	2.02	0.25	0.20	0.28
3/2$^+$	0.976 3/2$^+$ 2	1.69 (3/2)$^+$ 2	2.15	2.00	0.48	0.29	0.46
5/2$^+$	1.962 5/2$^+$ 2	3.48 or 4.15 (5/2$^+$) (2)	1.15	~0.6	0.21	~0.09	0.26
7/2$^+$	2.737 (7/2$^+$) (4)		0.11				...
9/2$^+$	4.055 (9/2$^+$) (4)		0.04				...
1/2(+)11, 1/2$^+$	2.565 1/2$^+$ 0	3.47 1/2$^+$ 0	0.85	~1.4	0.09	~0.16	0.47[c]
3/2$^+$	2.803 (3/2)$^+$ 2	3.76 or 3.78 (3/2$^+$) (2)	3.05	~5.8	0.44	~0.83	0.49
5/2$^+$	3.903 (5/2$^+$) (2)	4.55 (5/2$^+$) (2)	0.13	0.29	0.02	0.04	0.04
3/2(+)8, 3/2$^+$	...	0.984 (3/2$^+$) 2		4.10		0.73	0.96
5/2$^+$	...						0.04
1/2(−)14, 3/2$^-$	3.408 3/2$^-$ 1	3.56(3/2)$^-$ 1	5.66	6.49	0.66[d]	0.79[d]	0.43
7/2$^-$	3.969 (7/2$^-$) (3)	3.76 or 3.78 (7/2$^-$) (3)	5.19	~5.2	1.62[d]	~1.30[d]	0.43
1/2$^-$	4.270 (1/2)$^-$ 1	4.82 (1/2)$^-$ 1	1.59	2.53	0.20[d]	0.32[d]	0.01[e]

[a] Obtained as the ratio of the experimental to twice the single-particle cross section according to Eq. (13). The single-particle cross sections are from Table III, interpolated according to Eq. (3) containing the condition $B_n = Q + 2.225$ MeV.
[b] Nilsson values for $\eta = 4$.
[c] For $\eta = 2$ this value is 0.30, in better agreement with experiment.
[d] These values would be smaller if the single-particle cross sections were calculated using the binding energies of unperturbed single-particle levels $(1f_{7/2}, 1p_{3/2}, 1p_{1/2})$ of spherically symmetric potential instead of using the binding energies of the actual perturbed states.
[e] For $\eta = 2$ this value is 0.10 in much better agreement with experiment.

The second excited state (1.69 MeV) was observed to decay exclusively to the ground state, and the experimental limit for the unobserved transition to the first excited state (0.954 MeV) was estimated to be about 5%.

It has been found in the medium[15,26,27] and heavy[28] nuclei, that the (d,p) cross sections leading to low-lying states behave very regularly when passing from one even-even target to the next even-even isotope of the same element. In other words, the cross sections leading to the low-lying states with the same spin are approximately the same for the two isotopes with the neutron number differing by two. This same situation is expected also according to the rotational model, if the neutron is transferred to an orbit which is empty in both isotopes, and if the two isotopes have approximately the same deformation. Accordingly, we expect the level scheme of Mg^{27} to be essentially the same as that of Mg^{25} except for the lowest band 5/2(+)5 which should be absent with Mg^{27}. As the level scheme of Mg^{25} is well known and as the stripping cross sections agree with theoretical predictions, we might check our expectation by comparing the low-lying levels of Mg^{27} with the known rotational levels of Mg^{25} according to observed l values and stripping cross sections. This is done in Fig. 10 and Table VI. Table VI includes besides cross sections at $\theta_{c.m.} = 25°$ also the so-called experimental values of the coefficients $c_{Nlj}{}^2$, which were obtained according to Eq. (13) by dividing the experimental cross section at $\theta_{c.m.} = 25°$ with twice the single-particle cross section at the same angle. They are quoted to show the

[26] B. L. Cohen and R. E. Price, Phys. Rev. 121, 1441 (1961).
[27] B. Čujec, Phys. Rev. 131, 735 (1963).
[28] P. Mukherjee and B. L. Cohen, Phys. Rev. 127, 1284 (1962).

agreement with theoretical predictions of the Nilsson model.

The matching of Mg^{27} levels with Mg^{25} levels according to the observed l values and (d,p) cross sections is easy and in almost all cases unambiguous. Thus, the only reasonable way to parallel, e.g., the two $l=0$ levels of Mg^{27}, the ground state with the cross section 2.02 mb/sr and the 3.47-MeV state with cross section ~ 1.4 mb/sr, is to let the first one correspond to 0.584-MeV level of Mg^{25} with cross section 2.58 mb/sr, and the second one to the Mg^{25} level at 2.565 MeV with cross section 0.85 mb/sr. In this way, the sequence of matched energy levels is the same, the cross sections of matched levels differ only by $\sim 30\%$, while within the same isotope they differ by a factor of about two. Accordingly, the ground state of Mg^{27} is the 1/2$^+$ member of 1/2(+)9 band, and the level at 3.47 MeV is the 1/2$^+$ member of the 1/2(+)11 band. Similarly, there is no ambiguity with the two $l=1$ levels, the 1/2$^-$ and 3/2$^-$ members of the 1/2(−)14 band being thus well identified. The 7/2$^-$ member of the 1/2(−)14 band is very probably one of the levels at 3.78 MeV or 3.76 MeV. The two levels were not resolved in the present measurement and show combined an enormous cross section of 11 mb/sr and have an angular distribution characteristic of $l=3$ with the possibility of $l=2$ being also present (Fig. 7). This identification is supported by the fact that the only two levels which remained to be identified in this energy region and with high cross section are the 3/2$^+$ member of the 1/2(+)11 band and the 7/2$^-$ member of the 1/2(−)14 band. As for $l=2$ levels, the matching is again straightforward, except for the first excited state at 0.984 MeV, which will be discussed later. The 3/2$^+$ member of the 1/2(+)11 band is either the 3.76-MeV

level or the 3.78 MeV for the reasons just mentioned in connection with $7/2^-$ state. The $3/2^+$ and $5/2^+$ spin assignment to the two $l=2$ levels of $1/2(+)11$ band with both, Mg^{25} and Mg^{27} nuclei is supported by agreement between experimental and theoretical values for $c_{Nlj}{}^2$; the distinction between the two possibilities ($3/2^+$ and $5/2^+$) is very clear as the respective $c_{Nlj}{}^2$ values differ by an order of magnitude.

The appearance of weakly excited states in Mg^{27} [there are seven with cross section ≤ 0.08 mb/sr up to 4.82-MeV excitation energy (Fig. 10)] is easy to understand. Two of them are probably the $7/2^+$ and $9/2^+$ members of the band $1/2(+)9$, which appear also in Mg^{25} below 4.27 MeV. Some or all of the others may be due to coupling between the vibrational state of the Mg^{26} core and the single-particle states of the last neutron. Although such states are not present in Mg^{25} below 4.27 MeV, they can appear lower in Mg^{27}, as the first vibrational level in Mg^{26} is lower (at 2.94 MeV) than in Mg^{24} (at 4.23 MeV).

The Mg^{27} first excited state at 0.984 MeV needs special consideration. Its cross section is large (4.10 mb/sr), approximately equal to that of the Mg^{25} ground state (3.98 mb/sr), which is actually the maximum cross section for $l=2$, corresponding to $c_{Nlj}{}^2=1$. Following the procedure applied to all other strongly excited states, the 0.984-MeV state of Mg^{27} should correspond to the Mg^{25} ground state, which is the $5/2^+$ member of $5/2(+)5$ band. However, according to the simple Nilsson model, the orbit $5/2(+)5$ is full in Mg^{26} and therefore the band $5/2(+)5$ cannot be present in Mg^{27}. Nevertheless, as we know (see previous section), the Mg^{26} ground-state wave function does not consist of a pure $(5/2(+)5)^2$ configuration, but there is an admixture of 16% of $(1/2(+)9)^2$ configuration. Accordingly, we expect configuration mixing also in Mg^{27}. Assuming for the first excited state the spin $5/2^+$ and the wave function of the form

$$\psi(Mg_{0.984}{}^{27}) = \gamma(5/2(+)5)^2(1/2(+)9)$$
$$+ \delta(1/2(+)9)^2(5/2(+)5), \quad (16)$$

we obtain the largest spectroscopic factor for $Mg^{26}(d,p)$-Mg^{27}, $5/2^+$ transition if $\gamma^2 = 0.64$ and $\delta^2 = 0.36$, which is but one-third of the maximum possible value corresponding to $c_{Nlj}{}^2=1$. Thus, the first excited state cannot be understood as the result of configuration mixing given by Eqs. (15b) and (16). It is quite probable that one of the states at 3.48 or 4.15 MeV, with cross section ~ 0.6 mb/sr, which remained unidentified, is due to this configuration mixing. The next possible interpretation is that the first excited state of Mg^{27} is the $3/2^+$ member of the band $3/2(+)8$. The theoretical prediction for $c_{Nlj}{}^2$ is again very close to 1, in agreement with the observed cross section. There are also some reasons to expect that the properties of low-lying levels of Mg^{27} are similar to those of Si^{29}, as both nuclei have the same number of neutrons and differ only in the number of protons by two. The first excited state (1.277 MeV) of Si^{29} is known[2] to have spin and parity $3/2^+$; the corresponding (d,p) cross section for 15-MeV deuterons, as measured by Blair and Quisenberry,[29] is 4.0 mb/sr, the same as in the Mg^{27} case. Moreover, it has been suggested by Bromley et al.[30] that this Si^{29} level is the $3/2^+$ member of $3/2(+)8$ band. It is only somewhat hard to understand why the orbit $3/2(+)8$, which does not appear in Mg^{25} up to 4.3 MeV, would come so low in Mg^{27}. This would happen, if the deformation would change to a negative value, in which case the orbit $3/2(+)8$ would come below the orbit $1/2(+)11$. Such a drastic change in deformation from Mg^{25} to Mg^{27} would probably cause essential changes also in the coefficients $c_{Nlj}{}^2$, which are, however, not observed. To clear up this question, first of all the spins of the first and second excited states should be determined by a direct method, e.g., by measuring the proton-gamma angular correlations.

[29] A. G. Blair and K. S. Quisenberry, Phys. Rev. **122**, 869 (1961).
[30] D. A. Bromley, H. E. Gove, and A. E. Litherland, Can. J. Phys. **35**, 1057 (1957).